

The metallicity dependence of the CO \rightarrow H₂ conversion factor in $z \geq 1$ star forming galaxies¹

R.Genzel^{1,2}, L.J.Tacconi¹, F.Combes³, A.Bolatto⁴, R.Neri⁵, A.Sternberg⁶, M.C.Cooper⁷,
N.Bouché⁸, F.Bournaud⁹, A.Burkert^{10,11}, J.Comerford¹², P.Cox⁵, M.Davis¹³, N.M. Förster
Schreiber¹, S.Garcia-Burillo¹⁴, J.Gracia-Carpio¹, D.Lutz¹, T.Naab¹⁵, S.Newman¹³,
A.Saintonge^{1,15}, K.Shapiro¹⁶, A.Shapley¹⁷ & B.Weiner¹⁸

¹ Max-Planck-Institut für extraterrestrische Physik (MPE), Giessenbachstr.1, 85748 Garching, Germany

(genzel@mpe.mpg.de, linda@mpe.mpg.de)

² Dept. of Physics, Le Conte Hall, University of California, CA 94720 Berkeley, USA

³ Observatoire de Paris, LERMA, CNRS, 61 Av. de l'Observatoire, F-75014 Paris, France

⁴ Dept. of Astronomy, University of Maryland, College Park, MD 20742-2421, USA

⁵ IRAM, 300 Rue de la Piscine, 38406 St.Martin d'Herès, Grenoble, France

⁶ School of Physics and Astronomy, Tel Aviv University, Tel Aviv 69978, Israel

⁷ Hubble Fellow, Department of Physics & Astronomy, Frederick Reines Hall, University of California,
Irvine, CA 92697-4575, USA

⁸ Dept. of Physics, University of California, Santa Barbara, Broida Hall, Santa Barbara CA 93106, USA

⁹ Service d'Astrophysique, DAPNIA, CEA/Saclay, F-91191 Gif-sur-Yvette Cedex, France

¹⁰ Universitätssternwarte der Ludwig-Maximiliansuniversität, Scheinerstr. 1, D-81679 München, Germany

¹¹ MPG-Fellow at MPE

¹² Department of Astronomy & McDonald Observatory, 1 University Station, C1402 Austin, Texas 78712-
0259, USA

¹³ Department of Astronomy, Campbell Hall, University of California, Berkeley, CA 94720, USA

¹⁴ Observatorio Astronómico Nacional-OAN, Apartado 1143, 28800 Alcalá de Henares- Madrid, Spain

¹ Based on observations with the Plateau de Bure millimetre interferometer, operated by the Institute for Radio Astronomy in the Millimetre Range (IRAM), which is funded by a partnership of INSU/CNRS (France), MPG (Germany) and IGN (Spain).

¹⁵ *Max-Planck Institut für Astrophysik (MPA), Karl Schwarzschildstrasse 1, D-85748 Garching, Germany*

¹⁶ *Aerospace Research Laboratories, Northrop Grumman Aerospace Systems, Redondo Beach, CA 90278, USA*

¹⁷ *Department of Physics & Astronomy, University of California, Los Angeles, CA 90095-1547, USA*

¹⁸ *Steward Observatory, 933 N. Cherry Ave., University of Arizona, Tucson AZ 85721-0065, USA*

Abstract

We use the first systematic samples of CO millimeter line emission in $z\sim 1-3$ ‘main-sequence’ star forming galaxies (SFGs) for studying the metallicity dependence of the conversion factor α_{CO} , from CO millimeter line luminosity to molecular gas mass. The molecular gas depletion rate, which is proportional to the ratio of star formation rate to CO line luminosity, is $\sim 1 \text{ Gyr}^{-1}$ for near-solar metallicity galaxies with stellar masses above $M_{\text{S}} \sim 10^{11} M_{\odot}$. Its value does not vary much between $z\sim 0$ and 2. Below M_{S} the depletion rates appear to increase with decreasing metallicity. We show that this trend is probably not caused by starburst events or by changes in the physical parameters of the molecular clouds but instead requires a metallicity dependent conversion factor. The trend is also expected theoretically from the effect of UV-photodissociation of CO at low metallicity. From the available $z\sim 0$ and $z\sim 1-3$ samples we constrain the slope of the $\log(\alpha_{\text{CO}}) - \log(\text{metallicity})$ relation to range between -1.3 and -1.9. Because of the lower metallicities near and beyond the peak of the galaxy formation activity at $z\sim 1-2$ compared to $z\sim 0$, our findings suggest that molecular gas masses estimated from CO luminosities have to be substantially corrected upward for galaxies below M_{S} .

Subject Headings: galaxies: evolution – galaxies: high redshift – galaxies: ISM – stars: formation – ISM: molecules

1. Introduction

The evolution of galactic star formation as a function of cosmic time is driven by the complex interplay of interstellar gas components and their chemical evolution, stars and their radiation and feedback, star formation processes and galactic/intergalactic environments. In the Milky Way and nearby galaxies most or all star formation occurs in dense, cool giant molecular clouds (GMCs: Solomon et al. 1987, Young & Scoville 1991, Blitz 1993, McKee & Ostriker 2007, Bigiel et al. 2008, Leroy et al. 2008, Bolatto et al. 2008, Krumholz et al. 2011, Schruba et al. 2011). The most commonly used tracer of the H₂ molecule, the elusive building block of GMCs, is line emission from low-lying rotational transitions of ¹²CO. This is perhaps surprising since these transitions are quite optically thick ($\tau_{\text{CO } 1-0} \geq 10$) in typical GMCs. The information on gas mass/content is mainly contained in the width of the line if the gas motions are virialized (Dickman et al. 1986, Solomon et al. 1987). As a result the relationship between velocity integrated line flux $F_{\text{CO } J}$ (Jy km/s) in the $J \rightarrow J-1$ transition and total molecular gas mass (including 36% helium) on large scales is traditionally given by the empirical relation (Dickman et al. 1986, Downes et al. 1993, Downes & Solomon 1998, Appendix A in Tacconi et al. 2008, Obreschkow & Rawlings 2009)

$$M_{\text{gas}}/M_{\odot} = \alpha_{\text{CO } 1-0} L_{\text{CO } 1-0} = 1.75 \times 10^9 \left(\frac{\alpha_{\text{CO } 1-0}}{\alpha_G} \right) \left(\frac{F_{\text{CO } J}}{\text{Jy km/s}} \right) (R_{1J}) (1+z)^{-3} \left(\frac{\lambda_{\text{obs } J}}{\text{mm}} \right)^2 \left(\frac{D_L}{\text{Gpc}} \right)^2 \quad (1),$$

where

$$\alpha_{\text{CO } 1-0} = \alpha_G h \left(f_{\text{gas}}, \frac{(\langle n(\text{H}_2) \rangle)^{1/2}}{T_{R1}} \right) g(Z) \quad (2).$$

Here $L_{\text{CO } 1-0}$ (K km/s pc^2) is the integrated line luminosity of the 1-0 CO line, R_{1J} is the ratio of the Rayleigh-Jeans brightness temperatures T_{R}^2 of the $1 \rightarrow 0$ and the $J \rightarrow J-1$ transitions (at the same angular resolution), $\lambda_{\text{obs } J}$ is the observed wavelength of the $J \rightarrow J-1$ transition and D_{L} is the luminosity distance of the source. The functions h and g encapsulate the dependence of the function $\alpha_{\text{CO } 1-0}$ ($M_{\odot}/(\text{K km/s pc}^2)$, commonly called ‘conversion factor’) on physical conditions of the interstellar medium (ISM), and on metallicity Z . The conversion factor depends on the spatial distribution and mass fraction of the molecular gas in the cloud/galaxy (f_{gas}), as well as on the ratio of the mean hydrogen density $\langle n(\text{H}_2) \rangle$ and the Rayleigh-Jeans brightness temperature, and potentially on other parameters, such as the magnitude of turbulence in the GMCs etc. (Downes et al. 1993, Obreshkov et al. 2009, Tacconi et al. 2008, Pelupessy & Papadopoulos 2009, Shetty et al. 2011a,b, Shetty et al. 2011a,b, Narayanan et al. 2011). Since the penetration depth of external UV radiation destroying molecules depends on the extinction through the cloud, and thus on its metallicity, the optical depth and the effective conversion factor in CO transitions also depend on metallicity, especially in low metallicity, diffuse gas (van Dishoeck & Black 1986, 1988, Maloney & Black 1988, Sternberg & Dalgarno 1995, Hollenbach & Tielens 1999, Wolfire et al. 1990, 2010, Pelupessy & Papadopoulos 2009, Shetty et al. 2011a).

In the galaxy-integrated ISMs of the Milky Way and nearby SFGs with near solar metallicity, as well as in dense star forming clumps of lower mass, lower metallicity galaxies, the CO 1-0 conversion factors determined with dynamical, dust and γ -ray calibrations are consistent with a single value of $\alpha_{\text{G}} = 4.36 \pm 0.9 M_{\odot}/(\text{K km/s pc}^2)$ (Strong

² For a transition $J \rightarrow J-1$ at frequency ν_J , excitation temperature T_{ex} and optical depth τ_J the Rayleigh-Jeans brightness temperature is given by $T_{\text{RJ}} = h\nu_J/k (\exp(h\nu_J/(kT_{\text{ex}})-1))^{-1} (1-\exp(-\tau_J))$

& Maddox 1996, Dame, Hartmann & Thaddeus 2001, Grenier et al. 2005, Bolatto et al. 2008, Leroy et al. 2011, Abdo et al. 2011). In these environments GMCs appear to have similar physical properties and the functions h and g all take on values near unity (Bigiel et al. 2008, 2011, Leroy et al. 2008). In denser star forming regions or starburst galaxies the higher average densities drive $\alpha_{\text{CO } 1-0}$ upward. At the same time the increase in temperature due to stellar heating drives $\alpha_{\text{CO } 1-0}$ downward, fortuitously resulting in little change of $\alpha_{\text{CO } 1-0}$ even in these cases. More significant deviations of $\alpha_{\text{CO } 1-0}$ from the Galactic value occur in extreme merger-driven starbursts ($\alpha_{\text{CO } 1-0} \leq 1$, Solomon et al. 1997, Scoville et al. 1997, Downes & Solomon 1998, Tacconi et al. 2008). In low metallicity dwarf galaxies the Galactic conversion factor appears to underestimate the true molecular hydrogen content ($\alpha_{\text{CO } 1-0} > 1$), suggesting that in $z \sim 0$ SFGs $\alpha_{\text{CO } 1-0}$ scales with gas-phase oxygen abundance $\mu_{\text{O}} \equiv 12 + \log \{ \text{O}/\text{H} \}$ as $\mu_{\text{O}}^{-0.7 \dots -2}$ (Rubio, Lequeux & Boulanger 1993, Wilson 1995, Arimoto et al. 1996, Israel 1997, 2000, Boselli et al. 2002, Leroy et al. 2011, Bolatto et al. 2011).

In this paper we present a pilot study of the dependence of $\alpha_{\text{CO } 1-0}$ on metallicity, based on the first systematic measurements of CO emission in several samples of massive high-redshift ($z \sim 1-3$) SFGs. We find that the application of a Galactic conversion factor underestimates molecular masses in some of these systems by factors between 2 and 10. The outliers are low metallicity galaxies. We propose a first order empirical relation to correct the $\text{CO} \rightarrow \text{H}_2$ conversion factor at $z \geq 1$ for this metallicity effect.

2. Properties of the observed galaxies

2.1 Galaxy sample

In this paper we discuss recent galaxy integrated measurements of the ^{12}CO 3-2/2-1 lines in $z\sim 1-3$ ‘normal’ massive SFGs. The galaxies we are analyzing exhibit a reasonably tight correlation between stellar mass and star formation rate, or stellar mass and specific star formation rate ($\text{SSFR}=\text{SFR}/M_*$), the so called ‘star formation main-sequence’. The relation has a substantial scatter of rms 0.3dex (Figure 1, Elbaz et al. 2007, Noeske et al. 2007, Daddi et al. 2007, Rodighiero et al. 2010, Mancini et al. 2011). Galaxies near the ‘main sequence’ at redshifts from 0 to 2 have disk-like morphologies with low Sersic indices ($n\sim 1-2$) and, compared to off-main sequence systems, also have relatively large effective radii (Wuyts et al. 2011). Most of the galaxies in our sample are extended rotating disks and a few are compact, dispersion dominated systems (Förster Schreiber et al. 2009, Law et al. 2009, Tacconi et al. 2010, Daddi et al. 2010a, Mancini et al. 2001). Two galaxies (EGS 13004291, BX528) probably are major mergers (Förster Schreiber et al. 2009, Tacconi et al. 2010).

CO 3-2 and 2-1 observations for the galaxies in our sample are reported in Tacconi et al. (2010), Daddi et al. (2010a) and Tacconi & Combes et al. (in prep.) and were all observed with the IRAM Plateau de Bure millimetre Interferometer (Guilloteau et al. 1992). The Tacconi et al. (2010, and in prep.) galaxies (‘LP’) are drawn from two samples of $\langle z \rangle = 1.2$ and $\langle z \rangle = 2.3$ SFGs, matched to cover the same ranges of stellar mass ($M_*=3-30 \times 10^{10} M_\odot$) and star formation ($20-300 M_\odot \text{yr}^{-1}$). The current LP sample has 20 detections between $z=1$ and 1.5, and 11 detections and 5 upper limits between $z=2$ and 2.4. We also include 4 detections from Daddi et al. (2010a) at $\langle z \rangle = 1.5$, with comparable

selection criteria as in the LP sample. To these sets we finally add the detections of three somewhat lower mass ($M_* = 5-30 \times 10^9 M_\odot$), strongly lensed SFGs between $z \sim 2.3$ and 3.1 (cB58: Baker et al. 2004, ‘cosmic eye’: Coppin et al. 2007, ‘eyelash’: Swinbank et al. 2010, Danielson et al. 2010). For a description of the observations and the data analysis we refer to the papers above. We use a standard WMAP Λ CDM cosmology (Komatsu et al. 2011) and a Chabrier (2003) initial stellar mass function. To convert the 3-2 and 2-1 line fluxes to 1-0 fluxes we take $R_{I3} = 2$ and $R_{I2} = 1.16$ (Weiss et al. 2007, Dannerbauer et al. 2009, Ivison et al. 2011), with the exception of the more compact eyelash, where Danielson et al. (2010) find $R_{I3} = 1.5$ (see Genzel et al. 2010 for more details).

2.2 Metallicities

For 14 $z \geq 1$ SFGs we have individual determinations of gas phase metallicities based on the [NII]/H α estimator of Pettini & Pagel (2004: $\mu_O = 8.9 + 0.57 \log (F([\text{NII}])/F(\text{H}\alpha))$). The rms dispersion of the Pettini & Pagel relation is 0.18 dex for $7.5 < \mu_O < 8.6$. For the rest we determined metallicities from the stellar mass-metallicity relation at the respective redshifts (Erb et al. 2006b, Buschkamp et al. in prep., Shapley et al. 2005, Liu et al. 2008, $\mu_O = a + 2.18 \log(M_*) - 0.0896 \log(M_*)^2$, with $a = -4.51$ for $z = 1.5-3$, and $a = -4.45$ for $z \sim 1-1.5$). The rms dispersion of the $z \sim 2$ mass-metallicity relation is about 0.09 dex. The [NII]/H α ratio is known to saturate above roughly solar metallicity (e.g., Pettini & Pagel 2004), and systematic uncertainties between different metallicity indicators and calibrations can exceed 0.3 dex (e.g., Kewley & Ellison 2008). We converted all metallicities to the Denicolo, Terlevich & Terlevich (2002) calibration system (also based on [NII]/H α), with the conversion function given in Table 3 of Kewley & Ellison (2008).

The transformation onto the Denicolo et al. scale has the advantage that it delivers the best agreement between different metallicity calibrators. It optimizes the comparison to the $z \sim 0$ metallicity estimates, especially at the high M_* end (Kewley & Ellison 2008), which is particularly important for our study. The systematic uncertainties within the Denicolo et al. (2002) system and over the observed range should be within ± 0.2 dex (Kewley & Ellison 2008). Relative uncertainties from the measurement errors in $[\text{NII}]/\text{H}\alpha$ are much smaller (see typical red error bar at the bottom of Figure 2). For the 14 SFGs with metallicity estimates from both methods, the agreement is excellent with an rms scatter of 0.1 dex.

Our final sample of 43 $z \geq 1$ SFGs covers inferred oxygen abundances from $\mu_{\text{O}} \sim 8.4$ to 8.9 on the Denicolo et al. (2002) scale. The $z \sim 2$ sample includes two AGNs (Erb et al. 2006b), for which we adopt the metallicities estimated from the mass-metallicity relation. For comparison to $z \sim 0$ SFGs of different metallicities we used the recent compilations of Leroy et al. (2011) and Krumholz et al. (2011). However we replaced their quoted metallicities by $[\text{NII}]/\text{H}\alpha$ -based metallicities from the published literature, with the same calibrations as for the high- z data. Most of the $[\text{NII}]/\text{H}\alpha$ -derived metallicities are very similar to the ones given by Leroy et al. and Krumholz et al.

3. Results

3.1 The ratio $\text{SFR}/(\alpha_G L_{\text{CO } 1-0})$ increases with decreasing metallicity

Our basic method for exploring a metallicity dependence of the CO conversion factor in the $z \geq 1$ SFGs is to search for a systematic metallicity dependence in the Kennicutt-Schmidt relation ('KS', Kennicutt et al. 1998, 2007) between molecular gas and star formation rate, and relies on the universal properties of the KS-relation in massive SFGs at redshifts between 0 and 3. Recent studies of galaxy integrated or spatially resolved KS-relations in high-metallicity, non-merger SFGs near the star formation main-sequence and near solar metallicity have found that the star formation rate surface density, $\Sigma_{\text{star form}}$, depends on molecular gas surface density, $\Sigma_{\text{mol gas}}$, with a near-linear power-law ($\Sigma_{\text{SFR}} \propto \Sigma_{\text{mol gas}}^{1.0 \dots 1.2}$, Bigiel et al. 2008, Leroy et al. 2008, Daddi et al. 2010b, Genzel et al. 2010, Schruba et al. 2011). The relation is similar at low and high redshifts and includes also moderate $z \sim 0$ starbursts, such as M82 or NGC 253. This means that the ratio $\text{SFR}/(\alpha_G L_{\text{CO } 1-0}) = \text{SFR}/M_{\text{mol gas}}(\alpha_G)$ is effectively a molecular gas depletion rate, $(t_{\text{depletion}}(\text{CO}))^{-1}$. This depletion rate appears to be 0.4 to 0.5 Gyr^{-1} at $z \sim 0$ and $\sim 1 \text{ Gyr}^{-1}$ at $z = 1-2.5$ (Leroy et al. 2008, Bigiel et al. 2011, Tacconi et al. 2010, Daddi et al. 2010a,b, Genzel et al. 2010, Bauermeister et al. 2010). In normal star-forming $z \sim 0$ disks the maximum differences in depletion rates are ~ 0.5 dex (Saintonge et al. 2011). More extreme $z \sim 0-0.5$ starbursts, $z \sim 0$ ultra-luminous infrared galaxy mergers (ULIRGs) or $z \geq 1$ submillimeter galaxies have an order of magnitude larger depletion rates (Combes et al. 2011, Saintonge et al. 2011).

In the left panel of Figure 2 we plot $\text{SFR}/(\alpha_G L_{\text{CO } 1-0})$ as a function of gas phase oxygen abundance in the $z \sim 1-2.5$ SFGs of our sample. At or above solar metallicity all

$z \geq 1$ SFGs approach $\text{SFR}/\alpha_G L_{\text{CO } 1-0} \sim 1 \text{ Gyr}^{-1}$, in agreement with the discussion above, and with a scatter that is consistent with the measurement uncertainties. Below solar metallicity, the data exhibit a trend of rapidly increasing $\text{SFR}/\alpha_G L_{\text{CO } 1-0}$ with decreasing oxygen abundance. The trend at $z \geq 1$ is similar to that found at $z \sim 0$. Data points with metallicities derived from $[\text{NII}]/\text{H}\alpha$ and from the mass-metallicity relation agree well but the overall scatter is quite large.

3.2 The variation in $\text{SFR}/L_{\text{CO } 1-0}$ is not due to changes in physical gas depletion time or ISM conditions

Can this trend be driven by a physical change in depletion rate or in the ISM properties, and is metallicity the primary underlying variable? The lowest metallicity $z \sim 0$ star-forming systems are dwarf/irregular galaxies, such as the SMC and NGC 6822. Given the evidence for time variable star formation histories in such systems (Tolstoy, Hill & Tosi 2009) the order of magnitude or more larger depletion rates compared to normal disk galaxies might be the result of recent short-duration starbursts in the gas rich, low mass dwarfs. However, combined spatially resolved studies of HI, infrared dust and CO emission in the SMC and a number of the other $z \sim 0$ SFGs plotted in Figure 2 – allowing the derivation of gas depletion rates without relying on the KS-relation – strongly suggest that it is the absence of CO emission, and not the presence of starburst events that dominate the apparently high depletion rates (Leroy et al. 2011, Bolatto et al. 2011).

With the exception of cB58, the starburst explanation is even more unlikely to be applicable in general terms to the high- z SFGs in our sample. Almost all are massive

systems on or near the star formation main-sequence (Figure 1). Galaxies near the main sequence exhibit exponential light profiles with fairly large ($R_{1/2} \sim 3-6$ kpc) disk radii (Wuyts et al. 2011). They exhibit high star formation duty cycles (30-100 %, Adelberger et al. 2005, Noeske et al. 2007, Daddi et al. 2007). High- z main-sequence SFGs are forming stars at high rates ($20-300 M_{\odot} \text{yr}^{-1}$) because of the large gas accretion rates and high gas fractions typical in the high- z Universe (Daddi et al. 2010a, Tacconi et al. 2010, Bouché et al. 2010), and not necessarily because they are undergoing short-duration ‘starburst’ events. At fixed redshift the star formation surface densities are almost constant as a function of stellar mass (and thus metallicity) along the main-sequence ($\sim 0.5-3 M_{\odot} \text{yr}^{-1} \text{kpc}^{-2}$ for $z \sim 1-2$, Wuyts et al. 2011).

With the possible exception of the lensed ‘eyelash’ (Swinbank et al. 2010) all galaxies in our sample are within the ± 0.3 dex dispersion of the M^* -SSFR main sequence relations at $z \sim 1.2$ and 2.2 , including the individual uncertainties in stellar masses and star formation rates (Figure 1). Extreme merger induced starbursts (e.g. $z \sim 0$ ULIRGs) typically lie an order of magnitude or more above the main-sequence line.

Recent Herschel PACS observations have revealed a remarkable uniformity of the infrared spectral energy distributions of massive main-sequence SFGs at all redshifts (Hwang et al. 2010, Elbaz et al. 2011, Nordon et al. 2011). These measurements clearly show that main-sequence galaxies with star formation rates from a few to a few hundred solar masses per year (with the exception of $z \sim 0$ ULIRGs) have similar dust temperatures, $T_{\text{dust}} \sim 27-38$ K, between $z \sim 0$ and 2 (Hwang et al. 2010). High- z SFGs are 2-5 K colder than $z \sim 0$ SFGs of the same luminosity.

Observations of multiple CO rotational lines in a number of $z \geq 1$ SFGs and submillimeter galaxies find that the CO ladder distributions are similar to those of local starburst galaxies, such as M82 and NGC253, with inferred local molecular hydrogen volume densities (for the CO 3-2 emission) of $n_{\text{H}_2} = 10^{2.5 \dots 4.5} \text{ cm}^{-3}$ (Weiss et al. 2007, Dannerbauer et al. 2009, Danielson et al. 2010, Riechers et al. 2011). Average molecular hydrogen densities in the giant star forming clumps in $z \geq 1$ SFGs may be $\sim 10^{2 \dots 3} \text{ cm}^{-3}$ (Genzel et al. 2011). This means that the average ratio $\frac{(\langle n(\text{H}_2) \rangle)^{1/2}}{T_{\text{R}1}}$ in equation (2) probably is comparable in $z \geq 1$ SFGs to that in moderate $z \sim 0$ starbursts, or the Milky Way GMC population ($T_{\text{R}1} \sim 7\text{-}30 \text{ K}$, $\langle n_{\text{H}_2} \rangle \sim 10^{1.5 \dots 2} \text{ cm}^{-3}$). However, the fortuitous cancellation of the density and temperature dependencies may break down near massive star formation sites and plausibly drive the conversion factor downward, as in the case of the central starburst region in M82 ($\alpha_{\text{CO}1-0} \sim 2$, Wild et al. 1992, Weiss et al. 2001).

Could the large turbulence in high- z SFGs affect the observed metallicity trend in $\alpha_{\text{CO}1-0}$? As a rule $z \geq 1$ SFGs near the ‘main sequence’ exhibit 4 to 10 times larger velocity dispersions than $z \sim 0$ SFGs (Förster Schreiber et al. 2009, Law et al. 2009, Epinat et al. 2009). Recent theoretical work suggests that increased turbulence may profoundly affect the local density and temperature structure, and in turn also the conversion factor (Narayanan et al. 2011, Shetty et al. 2011a,b). However, the observed velocity dispersions in $z \geq 1$ main-sequence SFGs appear to depend little on galaxy mass, star formation rate or surface density (Genzel et al. 2011 and references therein). In addition, for most of the $z \geq 1$ SFGs in Figures 1 and 2 large scale rotation dominates over random motions, in contrast to many $z \sim 0$ ULIRGs and $z \geq 1$ submillimeter galaxies (Tacconi et al.

2008, Engel et al. 2010). Star formation in $z \geq 1$ main sequence SFGs is plausibly driven by gravitational instabilities in giant star forming clouds, similar to GMCs but scaled-up to the large gas fractions at $z \geq 1$ (Genzel et al. 2011). In any case the effect of turbulent compression and the presence of non-virialized gas components with chaotic motions drive the conversion factor downward, not upward, both in the empirical data (Solomon et al. 1997, Scoville et al. 1997, Downes & Solomon 1998, Tacconi et al. 1999, 2008), as well as in the simulations of Narayanan et al. (2011) and Shetty et al. (2011b).

Another issue is whether the CO rotational ladder excitation might vary between galaxies in a systematic way such that a constant brightness temperature scaling factor R_{1J} from J to 1, as used in this study, is not appropriate. The first studies of the CO rotational ladder distributions indeed show variations in CO rotational excitations but for $J \leq 3$ these are by far too small to account for the magnitude of the variations in Figure 2 (Weiss et al. 2007, Dannerbauer et al. 2009, Danielson et al. 2010, Riechers et al. 2011, Ivison et al. 2011). It is thus unlikely that the trend we observe in Figure 2 is caused by variations with galaxy mass or metallicity in the value of the function h in equation (2).

3.3 The variation in $\text{SFR}/L_{\text{CO } 1-0}$ may be caused by photodissociation of CO in low-metallicity environments

Figure 2 shows the images and spectra of two $z \sim 2$ SFGs at opposite extremes of the metallicity distribution of our sample, which otherwise have very similar star formation rates ($210\text{-}290 M_{\odot}\text{yr}^{-1}$), dynamical masses ($\geq 10^{11} M_{\odot}$), sizes ($R_{1/2} \sim 5\text{-}6$ kpc), as well as matter surface densities ($10^{2.5-3} M_{\odot}\text{pc}^{-2}$, Genzel et al. 2008, 2011). Both are clumpy rotating disks. Their stellar masses and metallicities differ by factors of 4 and 2.3,

respectively. Their CO 3-2 to extinction corrected H α flux ratios differ by 5.4. While the CO 3-2 line is well detected in BX610 ($\mu_0=8.8$) it is only marginally detected in ZC406690 ($\mu_0=8.4$). Likewise in the clumpy, rotating disk BX482 ($\mu_0=8.5$, SFR $\sim 100 M_{\odot} \text{yr}^{-1}$, $R_{1/2}=4.2$ kpc, Genzel et al. 2008, 2011, Förster Schreiber et al. 2009, 2011) the ratio of the 3σ upper limit in CO 3-2 to the extinction corrected H α flux is 3 times lower than in BX610. There is no indication that the physical parameters affecting the function h in equation (2) should be different between these systems.

Overall the evidence is strong that the difference between these three galaxies and the overall trend in SFR/ $L_{\text{CO } 1-0}$ with μ_0 in Figure 2 is not driven by a variation in gas depletion time scales or other physical properties of the ISM.

Theoretical work on UV-illuminated molecular clouds has predicted a strong dependence of $(t_{\text{depletion}}(\text{CO}))^{-1}$ on metallicity for more than two decades, especially in somewhat diffuse molecular gas (van Dishoeck & Black 1986, 1988, Maloney & Black 1988, Sternberg & Dalgarno 1995, Hollenbach & Tielens 1999, Wolfire et al. 1990, 2010, Bolatto, Jackson & Ingalls 1999, Shetty et al. 2011a). The short-dashed blue curve in Figure 2 (from Krumholz et al. 2011) is the result of calculating $(t_{\text{depletion}}(\text{CO}, Z))^{-1}$ for a spherical molecular cloud with constant column density ($\Sigma_{\text{gas}} \sim 85 M_{\odot} \text{pc}^{-2} \sim \langle \Sigma_{\text{gas}}(\text{GMC}, \text{MW}) \rangle$), and exposed to a diffuse UV radiation field with a ratio of UV energy density G_{UV} to gas density n_{H} similar to that in the solar neighborhood ($\langle G_{\text{UV}}/n_{\text{H}} \rangle \sim 1_{\text{sn}}$). The volume filling factor of molecular gas is assumed to be $f_{\text{V}} \sim 0.2$. This curve represents the ratio of the total H $_2$ column through the cloud to the H $_2$ column in which CO remains molecular, given the adopted UV radiation field and its density, clumpiness and total column (Wolfire et al. 2010). The depth of the CO-photodissociation zone is controlled

by dust ($A_{UV} \sim 1$) and thus scales directly with metallicity (e.g. van Dishoeck & Black 1986, 1988, Maloney & Black 1988, Sternberg & Dalgarno 1995, Wolfire et al. 2010). The $z \geq 1$ SFGs in Figure 1 have $\langle G_{UV} \rangle \sim 10^{2 \dots 3} G_{sn}$. Average ISM densities are also greater by about the same factor, such that the ratio is probably similar to that in the solar neighborhood. The onset of the up-turn in the blue-dashed curve in Figure 2 depends strongly on f_V . Model curves with larger f_V values than chosen by Krumholz et al. (2011) have up-turns at higher metallicity. For a homogeneous cloud the up-turn occurs at solar metallicity. In contrast the models predict that $(t_{\text{depletion}}(\text{H}_2))^{-1}$, the depletion rate based on the amount of molecular hydrogen in a cloud, is quite insensitive to metallicity, mainly because the H_2 molecule partially self-shields against UV-photodissociation (e.g. Federman, Glassgold & Kwan 1979).

The agreement of the theoretical predictions with the observations suggests that the trends seen in Figure 2, at both low and high redshifts, may be the consequence of the ratio of the volume and mass of molecular gas traced by CO (relative to that in H_2) decreasing rapidly at low metallicity due to photodissociation by the ambient UV-field (see Pelupessy & Papadopoulos 2009, Krumholz et al. 2011, Shetty et al. 2011b).

3.4 An empirical scaling relation for $\alpha_{\text{CO}}(\mu_0)$

We now turn the results in Figure 2 around and derive an empirical dependence of $\alpha_{\text{CO } 1-0}$ on metallicity, based on the assumption of a KS-scaling relation. For this purpose we use the fit to the $z \geq 1$ $\Sigma_{\text{mol gas}} - \Sigma_{\text{star form}}$ relation in Figure 3 of Genzel et al. (2010), updated for the additional $z \geq 1$ SFGs discussed here and omitting low metallicity galaxies,

$$M_{mol\ gas}(M_{\odot}) = 9.8 \times 10^8 SFR(M_{\odot} yr^{-1})^{0.9} R_{1/2}(kpc)^{0.2} \quad (3),$$

where $R_{1/2}$ is the half-light radius. For the near-main sequence $z \geq 1$ SFGs discussed in this paper the above relation gives gas similar to other proposed gas-star formation relations (Bouché et al. 2007, Kennicutt et al. 2007, Leroy et al. 2008, Daddi et al. 2010b, Genzel et al. 2010). In comparison to equation (3) the simpler assumption of a constant depletion time of 1 Gyr at $z > 1$ yields typically 5% larger gas masses for all but the most compact galaxies. The relation given in equation (8) of Genzel et al. (2010) yields half the masses, and that in Kennicutt et al. (2007) yields 23% smaller gas masses. These differences are all within the typical systematic uncertainties of the empirical KS-relation (± 0.3 dex, Kennicutt 1998, 2008, Genzel et al. 2010).

With the gas masses estimated from equation (3), Figure 3 shows the derived CO 1-0 conversion factor as a function of metallicity for our $z \geq 1$ sample. For comparison, we show estimates of $\alpha_{CO\ 1-0}$ of $z \sim 0$ SFGs by Leroy et al. (2011). We also indicate previous scaling relations for $z \sim 0$ SFGs, partially based on similar galaxies but employing different methods compared to the more detailed work of Leroy et al. (Wilson 1995, Arimoto et al. 1996, Israel 1997, 2000, Boselli et al. 2002). The Leroy et al. (2011) estimates of $\alpha_{CO\ 1-0}$ come from simultaneous parametric fitting of spatially resolved HI, CO and dust emission. They do not rely on the KS-relation. As expected from the discussion in the last section the CO \rightarrow H₂ conversion factor increases with decreasing metallicity.

The relations for low and high- z data sets are similar. If both the $z \sim 0$ points of Leroy et al. (2011) and the $z \geq 1$ SFGs are combined (treating 3σ upper limits as detections), the best linear fit $\log(\alpha_{\text{CO } 1-0}) - \mu_{\text{O}}$ data yields the relation

$$\log(\alpha_{\text{CO } 1-0}) = -1.3 (\pm 0.25) (12 + \log(\text{O}/\text{H}))_{\text{Denicolo 02}} + 12.1 (\pm 2.1) \quad (4),$$

where the quoted uncertainties are 2σ fit uncertainties for equal weights to all data points (because of the dominance of the systematic errors discussed above). A fit to only the $z \geq 1$ data yields a slope of $-1.9 (\pm 0.66)$ and zero point of $17 (\pm 5.8)$, which is somewhat steeper than, but not significantly different from the combined fit. Our method constrains the relative conversion factor-metallicity relation to no better than $\pm 50\%$, since the rms scatter of the data points around any of the two relations given above is 0.23 dex. Absolute uncertainties are larger because of the inherent uncertainties in the metallicity calibrations, stellar masses and star formation rates. These uncertainties reflect a combination of the systematic uncertainties and plausible physical variations.

4. Conclusions

We have analyzed the empirical evidence for a metallicity dependence of the CO luminosity to molecular gas mass conversion factor $\alpha_{\text{CO } 1-0}$, based for the first time on both low- and high-redshift star forming galaxies. We find that the molecular gas mass depletion rate at both low and high redshift increases with decreasing gas phase

metallicity estimated from strong rest-frame optical emission line ratios. We interpret this trend as being mainly driven by the dependence on metallicity of the ratio of galaxy averaged, gas column traced by CO emission to the total H₂ column, consistent with the expectations from photodissociation region theory.

We then employed the KS- relation for high metallicity, near-main sequence SFGs at $z \geq 1$ for deriving empirical CO conversion factors. Combining our sample of 43 $z \geq 1$ SFGs with KS-independent conversion factors for 11 $z \sim 0$ SFGs from the compilation by Leroy et al. (2011) we find that the $\log(\alpha_{\text{CO } 1-0}) - (12 + \log\{\text{O}/\text{H}\})$ relation has a slope between -1.3 and -1.9. At 0.5 (respectively 0.25) times solar metallicity $\alpha_{\text{CO } 1-0}$ is ~ 2.5 to 4 times (respectively 6 to 14 times) larger than at solar metallicity. The uncertainties of the inferred $\alpha_{\text{CO } 1-0}$ values are 0.23 dex statistically and larger systematically, and are driven by the large measurement and calibration uncertainties, our small galaxy samples and potentially additional ‘hidden’ parameters and dependencies. Because of the obvious importance of the functional dependence of the CO conversion factor on metallicity and ISM parameters for future large molecular gas surveys it is highly desirable to improve the statistical robustness and uncertainties of the present result by enlarging the samples and their parameter ranges, in order to be able to better marginalize over these other parameters.

The implications of our findings may be particularly relevant for redshifts near and above the peak of cosmic star formation activity ($z \sim 1-2.5$). Because of the cosmic evolution of the mass-metallicity relation a galaxy at the knee of the stellar mass function ($M_{\text{S}} \sim 10^{11} M_{\odot}$) has ~ 0.74 , 0.69 and 0.55 solar metallicity at $z \sim 1$, 2.2 and 3.5 (Maiolino et al. 2008). A $0.1 M_{\text{S}}$ galaxy has typically half of the metallicity of an M_{S} galaxy. These

numbers immediately show that gas mass measurements may need to be significantly revised upwards at $z > 1$ even for $0.7 M_{\odot}$ galaxies, and $\leq 0.1 M_{\odot}$ galaxies at $z > 2$ may become hard to detect even with the superior sensitivity of ALMA.

References

- Abdo, A.A. et al. 2010, *ApJ* 710, 133
- Adelberger, K. L., Steidel, C. C., Pettini, M., Shapley, A. E., Reddy, N. A. & Erb, D. K. 2005, *ApJ* 619, 697
- Arimoto, N., Sofue, Y. & Tsujimoto, T. 1996, *PASJ* 48, 275
- Baker, A., Tacconi, L.J., Genzel, R., Lehnert, M.D. & Lutz, D. 2004, *ApJ* 604, 125
- Bauermeister, A., Blitz, L. & Ma, C.-P. 2010, *ApJ* 717, 323
- Bigiel, F., Leroy, A., Walter, F., Brinks, E., de Blok, W. J. G., Madore, B. & Thornley, M. D. 2008, *AJ* 136, 2846
- Bigiel, F. et al. 2011, *ApJ* 730, L13
- Blitz, L. 1993, in *Protostars & Planets III*, A93-42937 17-90, p. 125
- Bolatto, A.D., Jackson, J. M. & Ingalls, J. G. 1999, *ApJ* 513, 275
- Bolatto A.D., Leroy A. K., Rosolowsky E., Walter F., Blitz L., 2008, *ApJ* 686, 948
- Bolatto, A.D. et al. 2011, submitted to *ApJ*
- Boselli, A., Lequeux, J. & Gavazzi, G. 2002, *Ap&SS* 281, 127
- Bouché, N. et al. 2007, *ApJ* 671, 303
- Bouché, N. et al. 2010, *ApJ* 718, 1001
- Chabrier G., 2003, *PASP* 115, 763
- Combes, F., García-Burillo, S., Braine, J., Schinnerer, E., Walter, F. & Colina, L. 2011, *A&A* 528, 124
- Coppin, K.E.K. et al. 2007, *ApJ* 665, 936
- Daddi E. et al. 2007, *ApJ* 670, 156
- Daddi, E. et al. 2010a, *ApJ* 713, 686

Daddi, E. et al. 2010b, *ApJ* 714, L118

Dame T. M., Hartmann D.& Thaddeus P., 2001, *ApJ* 547, 792

Danielson, A.L.R. et al. 2011, *MNRAS* 410, 1687

Dannerbauer, H., Daddi, E., Riechers, D. A., Walter, F., Carilli, C. L., Dickinson, M.,
Elbaz, D. & Morrison, G. E. 2009, *ApJ* 698, L178

Denicoló, G., Terlevich, R. & Terlevich, E. 2002, *MNRAS* 330, 69

Dickman, R. L., Snell, R. L. & Schloerb, F. P. 1986, *ApJ* 309, 326

Downes, D. & Solomon, P. M. 1998, *ApJ* 507, 615.

Downes, D., Solomon, P.M. & Radford, S.J.E. 1993, *ApJ* 414, L13

Elbaz, D. et al. 2007, *A&A* 468, 33

Elbaz, D. et al. 2011, arXiv1105.2537

Engel, H. et al. 2010, *ApJ* 724, 233

Epinat, B. et al. 2009, *A&A* 504, 789

Erb D. K., Shapley A.E., Pettini M., Steidel C.C., Reddy N.A. & Adelberger K.L. 2006a,
ApJ 644, 813

Erb D. K., Steidel C.C., Shapley A. E., Pettini M., Reddy N. A. & Adelberger K. L. 2006b,
ApJ 647, 128

Federman, S. R., Glassgold, A. E.& Kwan, J. 1979, *ApJ* 227, 466

Förster Schreiber N. M. et al. 2009, *ApJ* 706, 1364

Förster Schreiber, N. M., Shapley, A. E., Erb, D. K., Genzel, R., Steidel, C. C., Bouché, N.,
Cresci, G. & Davies, R. 2011, *ApJ* 731, 65

Genzel, R. et al. 2008, *ApJ* 687, 59

Genzel, R. et al. 2010, *MNRAS* 407, 2091

Genzel, R. et al. 2011, *ApJ* 733, 101

Grenier, I. A., Casandjian, J.-M. & Terrier, R. 2005, *Sci* 307, 1292

Guilloteau S. et al. 1992, *A&A* 262, 624

Hollenbach, D. J.& Tielens, A. G. G. M. 1999 *RvMP* 71, 173

Hwang, H.S. et al. 2010, *MNRAS* 409, 75

Israel, F.P. 2000, in ‘Molecular Hydrogen in Space’, Eds. F.Combes & G.Pineau de Forêts, Cambridge : Cambridge Univ.Press, 326

Israel, F.P. 1997 *A&A* 328, 471

Iverson, R. J., Papadopoulos, P. P., Smail, I., Greve, T. R., Thomson, A. P., Xilouris, E. M. & Chapman, S. C. 2011, *MNRAS* 412, 1913

Kennicutt R. C., Jr. et al., 2007, *ApJ* 671, 333

Kennicutt, R. C., Jr. 1998, *ARAA* 36, 189

Kennicutt, R.C., Jr. 2008, *ASPC* 390, 149

Kewley, L.J. & Ellison, S.L. 2008, *ApJ* 681, 1183

Komatsu, E. et al. 2011, *ApJS* 192, 18

Krumholz, M. R., Leroy, A. K.& McKee, C. F. 2011, *ApJ* 731, 25

Law, D. R., Steidel, C. C., Erb, D. K., Larkin, J. E., Pettini, M., Shapley, A. E. & Wright, S. A. 2009, *ApJ* 697, 2057

Leroy A. K., Walter F., Brinks E., Bigiel F., de Blok W. J. G., Madore B., Thornley M. D. 2008, *AJ* 136, 2782

Leroy, A.K. et al. 2011, arXiv1102.4618

Liu, X., Shapley, A. E., Coil, A. L., Brinchmann, J. & Ma, C.-P. 2008, *ApJ* 678, 758

Maiolino, R. et al. 2008, *A&A* 488, 463

Maloney, P. & Black, J.H. 1988, *ApJ* 325, 389

Mancini, C., et al., 2011, *ApJ* submitted

McKee C. F. & Ostriker E. C., 2007, *ARA&A* 45, 565

Narayanan, D., Krumholz, M., Ostriker, E. C. & Hernquist, L. 2011, arXiv1104.4118

Noeske K. G. et al., 2007, *ApJ* 660, L43

Nordon, R. et al. 2011, arXiv1106.1186

Obreschkow D. & Rawlings S., 2009, *MNRAS*, 394, 1857

Pelupessy, F. I. & Papadopoulos, P. P. 2009, *ApJ* 707, 954

Pettini, M. & Pagel, B.E.J. 2004, *MNRAS* 348, L59

Riechers, D. A., Hodge, J., Walter, F., Carilli, C. L. & Bertoldi, F. 2011, arXiv1105.4177

Rodighiero, G. et al. 2010, *A&A* 518, L25

Rubio, M., Lequeux, J. & Boulanger, F. 1993, *A&A* 271, 9

Saintonge, A. et al. 2011, *ApJ* in press (arXiv1104.0019)

Schruba, A. et al. 2011, arXiv1105.4605

Scoville N. Z., Yun M. S. & Bryant P. M. 1997, *ApJ* 484, 702

Shapley, A.E., Coil, A.L., Ma, C.-P. & Bundy, K. 2005, *ApJ* 635, 1006

Shetty, R., Glover, S. C., Dullemond, C. P. & Klessen, R. S. 2011a, *MNRAS* 412, 1686

Shetty, R., Glover, S. C., Dullemond, C. P., Ostriker, E. C., Harris, Andrew I. & Klessen, R. S. 2011b, arXiv1104.3695

Solomon P. M., Downes D., Radford S. J. E. & Barrett J. W. 1997, *ApJ* 478, 144

Solomon P. M., Rivolo A. R., Barrett J. & Yahil, A., 1987, *ApJ* 319, 730

Sternberg, A. & Dalgarno, A. 1995, *ApJS* 99, 565

Strong A. W. & Mattox J. R., 1996, *A&A* 308, L21

Swinbank, A.M. et al. 2010, *Nature* 464, 733

Tacconi, L. J., Genzel, R., Tecza, M., Gallimore, J. F., Downes, D. & Scoville, N. Z.
1999, *ApJ* 524, 732

Tacconi L. J. et al. 2010, *Nature* 463, 781

Tacconi L. J. et al. 2008, *ApJ* 680, 246

Tolstoy, E., Hill, V. & Tosi, M. 2009, *ARAA* 47, 371

van Dishoeck, E.F. & Black, J.H. 1986, *ApJS* 62, 109

van Dishoeck, E.F. & Black, J.H. 1988, *ApJ* 334, 771

Weiss, A., Neininger, N., Hüttemeister, S. & Klein, U. 2001, *A&A* 365, 571

Weiss, A., Downes, D., Walter, F. & Henkel, C. 2007, *ASPC* 375, 25

Wild, W., Harris, A. I., Eckart, A., Genzel, R., Graf, U. U. & Jackson, J. M.,
Russell, A. P. G. & Stutzki, J. . 1992, *A&A* 265, 447

Wilson, C.D. 1995, *ApJ* 448, L97

Wolfire, M., Hollenbach, D.J. & Tielens, A.G.G.M. 1990, *ApJ* 358, 116

Wolfire, M. G., Hollenbach, D. & McKee, C. F. 2010, *ApJ* 716, 1191

Wuyts, S. et al. 2011, submitted

Young, J. S. & Scoville, N. Z. 1991, *ARAA* 29, 581

Figures

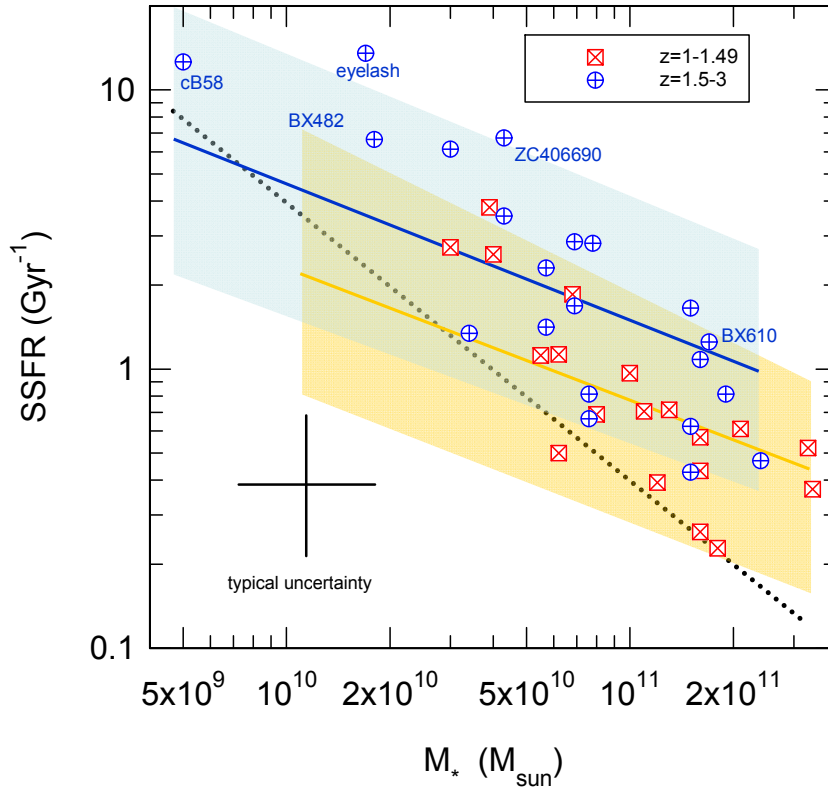


Figure 1. Specific star formation rate as a function of stellar mass for the $z=1-1.4$ SFGs (open crossed red squares) and $z=1.5-3$ SFGs (open crossed blue circles) of our sample. The orange and blue shaded regions (and orange and blue lines) denote the location of the ‘main-sequence’ at these redshifts, as determined from Noeske et al. (2007), Rodighiero et al. (2010), Förster Schreiber et al. (2009) and Mancini et al. (2011). The dotted line denotes the LP survey limit in star formation rate ($\text{SFR} \sim 40 M_{\odot} \text{yr}^{-1}$).

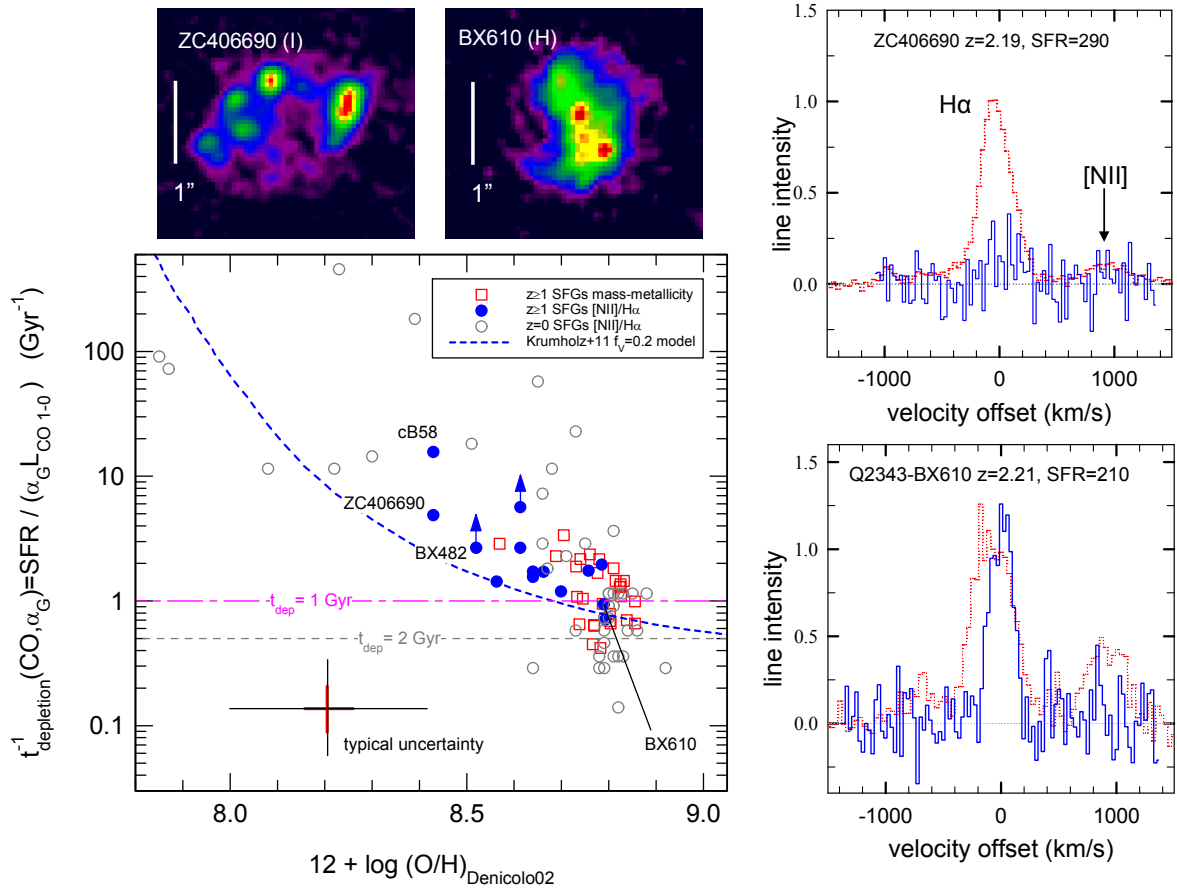


Figure 2. Dependence of the molecular gas depletion rate for a Galactic conversion factor (including helium), $(t_{\text{depletion}}(\text{CO}, \alpha_G))^{-1} = \text{SFR}/(\alpha_G L_{\text{CO } 1-0})$, on gas phase oxygen abundance (bottom left panel). The molecular gas mass is inferred from the observed CO 3-2/2-1 flux/luminosity from equations (1) and (2) with $R_{13}=2$ (1.5 for the eyelash) or $R_{12}=1.16$, and $\alpha_{\text{CO } 1-0}=\alpha_G=4.36$. The blue filled circles denote CO detections or 3σ upper limits of $z=1-2.5$ SFGs with individual determinations of the oxygen abundance based on the [NII]/H α ratio, the Pettini & Pagel (2004) relation ($\mu_0 = 12 + \log(\text{O}/\text{H})=8.9 + 0.57 \log(F([\text{NII}]/F(\text{H}\alpha)))$), and then converted to the Denicolo et al. (2002) calibration scale by using the conversion functions given in Kewley & Ellison (2008). The open red squares mark CO detections/upper limits with metallicities inferred from the stellar mass-

metallicity relation of Erb et al. 2006a, Liu et al. 2008 and Buschkamp et al. 2011 in prep.), again converted to the Denicolo et al. scale as described above. Open grey circles denote the compilation of $z\sim 0$ SFGs from Krumholz, Leroy & McKee (2011), for which metallicities were derived from $[\text{NII}]/\text{H}\alpha$ ratios in the literature, and then again converted to the Denicolo et al. (2002) calibration as described above. The best fit depletion time scales for near solar metallicity SFGs are $t_{\text{depletion}}\sim 2$ Gyr at $z\sim 0$ (Bigiel et al. 2008, 2011, Leroy et al. 2008) and ~ 1 Gyr at $z\sim 1-2.5$ (Tacconi et al. 2010, this paper), which are shown as dashed horizontal lines. The large cross at the bottom denotes the typical statistical (red) and systematic (black) rms errors. The blue dashed line is a theoretical prediction of the dependence of $(t_{\text{depletion}})^{-1}$ on μ_{O} for a molecular cloud of constant column density similar to that in Milky Way GMCs ($\sim 85 M_{\odot} \text{ pc}^{-2}$, $N(\text{H})=7.5\times 10^{21} \text{ cm}^{-2}$) and a ratio of UV radiation field to density similar to that in the solar neighbourhood (Krumholz et al. 2011). The top and right insets show the rest-frame UV/optical stellar images (Genzel et al. 2011, Förster Schreiber et al. 2011), $\text{H}\alpha/[\text{NII}]$ (dotted red, Genzel et al. 2011, Förster Schreiber et al. 2009) and CO 3-2 spectra (continuous blue, this paper) for two massive $z\sim 2$ SFGs of similar dynamical mass and star formation rate but different metallicities (and stellar masses), at the extremes of the observed distribution. The CO 3-2 and $\text{H}\alpha/[\text{NII}]$ spectra are normalized such that they both have a peak normalized intensity of unity for BX610. The low metallicity SFG ZC406690 has 5.4 times smaller CO to $\text{H}\alpha$ flux ratio than the high metallicity SFG BX610.

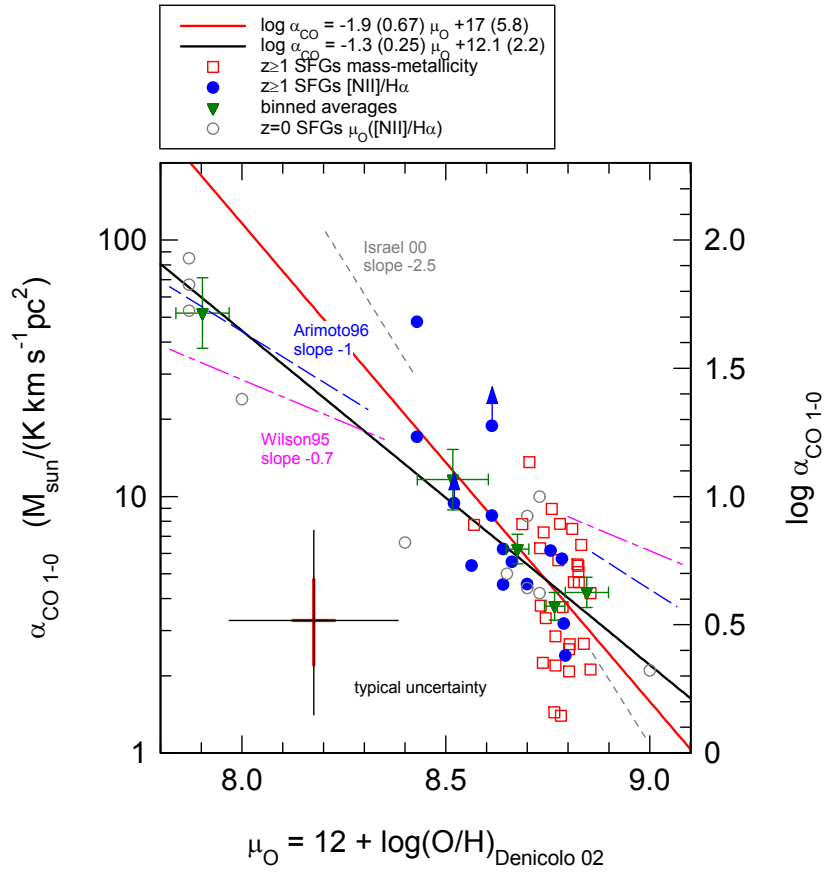


Figure 3. Inferred dependence of the CO 1-0 luminosity to molecular gas mass, conversion factor ($\alpha_{\text{CO } 1-0}$) on gas phase oxygen abundance. The molecular gas mass (including helium) for the high- z galaxies is computed from the best-fit $z \geq 1$ KS-relation (updating the data in Genzel et al. 2010 with the additional SFGs in Tacconi & Combes,

2011 (in prep) and selecting SFGs with $\mu_{\text{O}} \geq 8.7$: $\log \Sigma_{\text{star formation}} (\text{M}_{\odot} \text{yr}^{-1} \text{kpc}^{-2}) = 1.11 \log \Sigma_{\text{mol gas}} (\text{M}_{\odot} \text{pc}^{-2}) - 3.24$. The symbols for the high- z data points are the same as in Figure 2. Grey circles denote the determinations of $\alpha_{\text{CO } 1-0}$ from joint fits to spatially resolved HI, CO and dust data in $z \sim 0$ SFGs by Leroy et al. (2011). Green triangles denote average values from the combination of $z \sim 0$ and $z \geq 1$ data (and their dispersion in μ_{O} , and uncertainty in the mean in $\log(\alpha_{\text{CO } 1-0})$ in different metallicity bins. The large black (red) cross in the lower right denotes the typical systematic (statistical) rms errors. The trends of the Leroy et al. sample are in broad agreement with earlier work Wilson (1995, magenta long dashes), Arimoto et al. (1996, long-short black dashes) and Israel (2000, grey dots). The best linear fit in the $\log(\alpha_{\text{CO } 1-0})$ - $\log(\text{metallicity})$ plane to the all $z \sim 0$ and $z > 1$ SFGs is given by the continuous black line: $\log \alpha_{\text{CO } 1-0} = 12.1 (\pm 2.2) - 1.3 (\pm 0.26) \mu_{\text{O}}$, where the quoted errors are 2σ statistical fit uncertainties. The best fit to only $z \geq 1$ SFGs is given by the continuous red line: $\log \alpha_{\text{CO } 1-0} = 17 (\pm 5.8) - 1.9 (\pm 0.66) \mu_{\text{O}}$.